

U_{ZK} . The load R_0, L_0 is connected to the center A of the main half bridge and to $U_{ZK}/2$. The circuitry on the left side of the main module S_A is the ZCS-ARCP. Because only half-bridge modules were available in the laboratory, the resonant tank L_R, C_R is switched on half the DC-link voltage $U_{ZK}/2$ via the auto transformer Tr and the auxiliary half bridge S_H, D_H . The resonant inductor L_R is realised with the stray inductance of the auto transformer. The functioning of the ZCS-ARCP as well as the test circuit has been previously described in papers.

For the laboratory circuit in figure 1. the following compo-

nents and parameters have been selected:

- $U_{ZK} = 600V$
- $R_0 = 90m\Omega$
- $D_{K1}, D_{K2} - BY255 (ITT)$
- $D_{KP}, D_{KN} - BYT230PI-800 (ST)$
- $S_H, D_H - BSM50GB100D (Siemens)$
- $S_A, D_A - MG100Q2YS1 (Toshiba)$
- Auto transformer - $N = 10$,
- two ferrite pairs of E65 cores
- $L_R = 3,6mH$
- $C_R = 4.68nF (FKP1-cap., Wima)$
- $f_S = 17kHz$

The module S_A under test is mounted on a separate heat sink being held at $110^\circ C$ by a heater. The test circuit is operated in the burst mode such that the

chip temperature is only marginally above the heat sink temperature of about $100^\circ C$. Initially, the 100A, 1000V module BSM100GB100D is used. Figure 3 shows the voltage u_a across the switch, the switch current i_N , load current i_A and gate voltage $u_{gH,N}$ of the auxiliary switch; by its turn-on the quenching of the main switch is initiated. The load current is measured with a balanced shunt. By checking the measurements of the load current i_A with a Tektronix 100A current probe the temperature offset of the copper shunt is eliminated for determining the switching losses. As turn-off current I_{off} the amplitude of the load current i_A is used.

The snubber effect E is defined as:

$$E = 1 - \frac{W_{off,sn}}{W_{off,hard}} \quad (1)$$

Then the application of the snubber results in a reduction of the turn-off loss

$$P_{off,hard} = f_S \cdot W_{off,hard} \text{ by } E \cdot P_{off,hard}$$

Figure 2 shows the commutation of the main switch from BSM100GB100D down to the level of the tail current (about 12A). Channel two shows the gate signal of the main switch being turned off. An earlier turn off would only lead to higher losses and does not reduce the tail current. The turn-off current amounts to about 84A (20A/Div.).

$$W_{off,sn}(600V, 80A) \cong \frac{600 \cdot 80}{610 \cdot 84} \cdot \sum_{i=1}^5 W_{off,i} = 7mJ \quad (2)$$

In comparison, Figure 3 shows the turn-off process for about 81A without snubber.

$$W_{off,tail}(600V, 80A) \cong \frac{80}{84} \cdot \sum_{i=3}^6 W_{off,i} \cong 6,1mJ \quad (3)$$

$$W_{off,hard}(600V, 80A) \cong \frac{80}{74} \cdot \sum_{i=1}^6 W_{off,i} \cong 14,8mJ \quad (4)$$

The measurement for BSM100GB170D is performed with 600V. For this purpose, already the triggering level for the desaturation control (short circuit protection!) had to be increased; for the bottom switch it had to be eliminated completely. This switch carries a current pulse for charging up the quenching capacitor (cf. figure 4) at the first turn-on of the burst. The NPT-module goes into saturation more slowly than a PT-type.

Figure 4 shows the turn-on process and the saturation of the power switch (forward voltage u_F in channel 2), occurring 3 microseconds later. The intelligent gate driver circuit starts monitoring u_F 2 microseconds after turn-on.

$$W_{off,sn}(600V, 80A) \cong \sum_{i=1}^3 W_{off,i} = 9,8mJ \quad (5)$$

For exact determination of the switching losses and for separation into edge and tail losses for hard switching, the switching process shown in Figure 5 has been decompressed in time once more. The time interval 1T, starting after settling down of the switching overvoltage, is already attributed to the tail losses.

$$W_{off,Tail}(600V, 80A) \cong W_{offS,T} + \sum_{i=1}^3 W_{offT,i} = 9mJ \quad (6)$$

$$W_{off,hard}(600V, 80A) \cong \sum_{i=1}^7 W_{offS,i} + \sum_{i=1}^3 W_{offT,i} \cong 14,9mJ \quad (7)$$

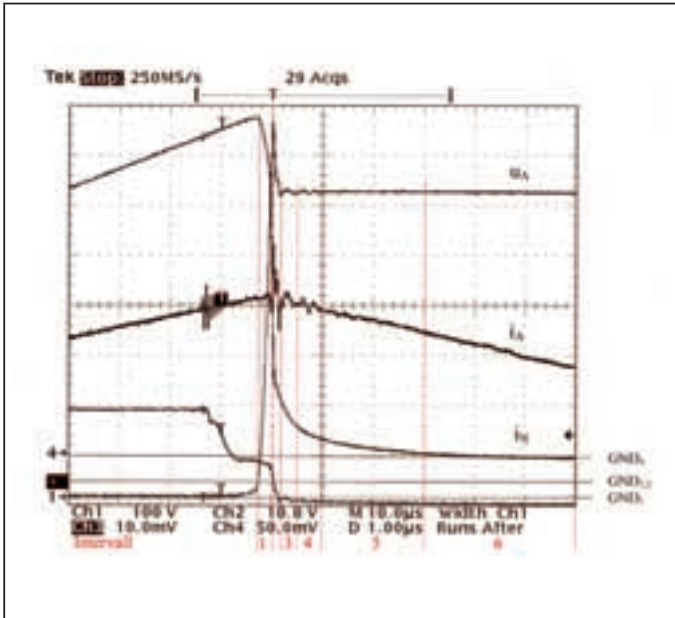


Figure 3: BSM100GB100 D; hard turn-off $I_{off} = 81A, U_{ZK} = 600V, T_j = 110^\circ C$

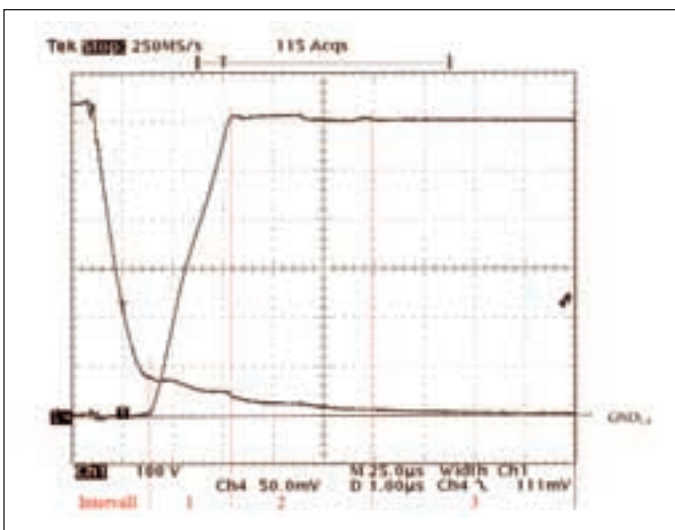


Figure 4: BSM100GB170D resonant turn-off, $I_{off} = 80A, U_{ZK} = 600V, T_j = 110^\circ C$

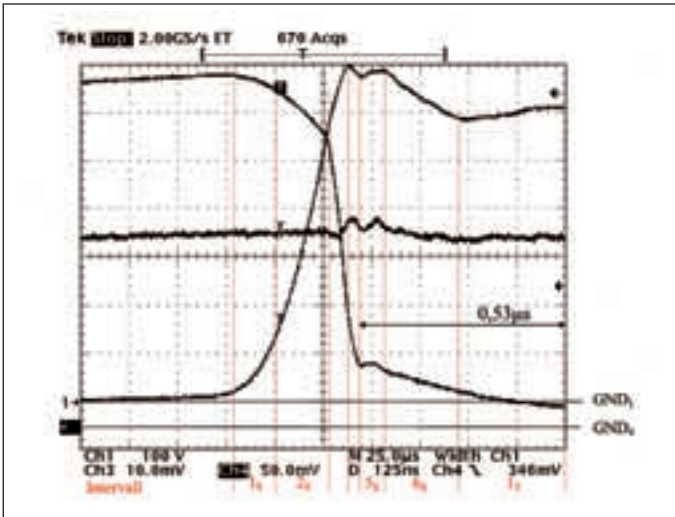


Figure 5: BSM100GB170D; hard turn-off $I_{off} = 87A$, $U_{ZK} = 600V$, $T_J = 110^\circ C$; determination of the loss contributions W_{offs} during the switching edges

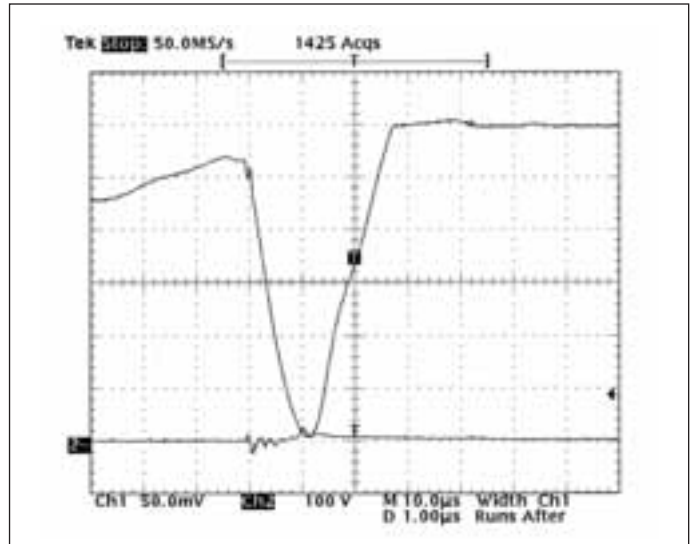


Figure 6: MG100Q2YS9; resonant turn-off, $I_{off} = 74A$, $U_{ZK} = 600V$, $T_J \approx 21^\circ C$

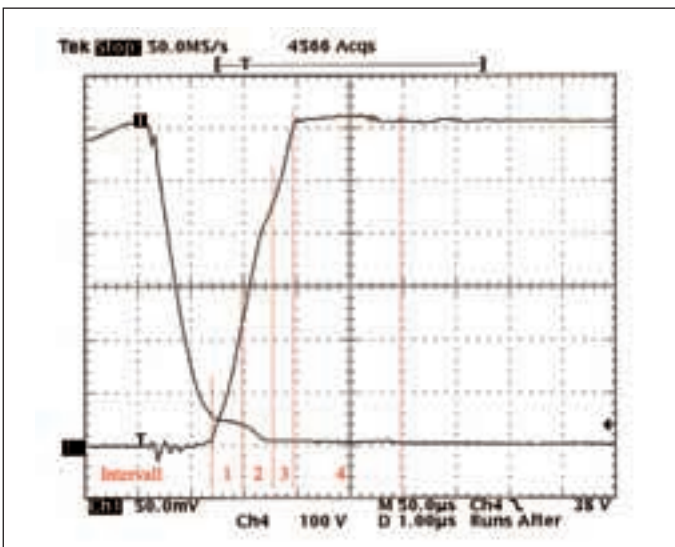


Figure 7: MG100Q2YS9; resonant turn-off, $I_{off} = 84A$, $U_{ZK} = 610V$, $T_J = 100^\circ C$

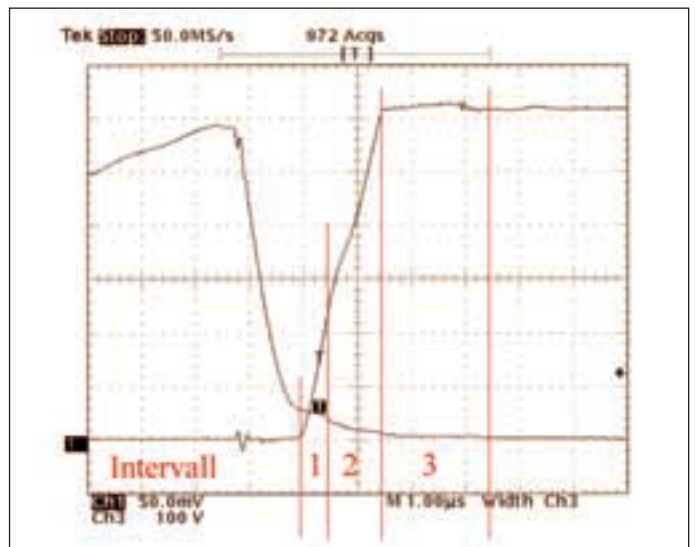


Figure 8: FF150R12KS4 ENG; resonant turn-off; $I_{off} = 81A$, $U_{ZK} = 610V$, $T_J = 21^\circ C$

$$W_{off,s}(600V, 80A) \approx \sum_{i=1}^6 W_{offs,i} = 5.9mJ \quad (8)$$

The currents of the power switches of the PT-IGBT module MG100Q2YS9 are also commutated down to the level of the tail current.

$$W_{off,entl} \approx 0mJ \quad (9)$$

To show the strong dependency of the tail current of PT-type IGBTs on the chip temperature, the cooler was not heated in

figure 6. Obviously, no tail current and no switching losses, respectively appear in this case.

High switching frequencies (around and above the upper audible frequency) can already be obtained without substantial increase of the switching losses. One can easily imagine that this switching frequency limitation can also be overcome in the future. Smallest intelligent snubbers for almost infinitely fast switches could reduce du/dt and di/dt to currently manageable switching speeds; these could then be easily handled due to small construction dimensions. Due to the heated cooler the chip temperature in figure 7 is about $100^\circ C$.

$$W_{off,sn}(600V, 80A) \approx \frac{600 \cdot 80}{610 \cdot 84} \cdot \sum_{i=1}^5 W_{off,i} = 2,3mJ \quad (10)$$

The current of the power switch of the NPT-IGBT module FF150R12KS4 - ENG is also commutated down to the level of its tail current.

$$W_{off,sn}(600V, 80A) \approx \frac{600 \cdot 80}{610 \cdot 81} \cdot \sum_{i=1}^5 W_{off,i} = 3mJ \quad (11)$$

The resonant turn-off losses of the chip (operated at about

16kHz) at room temperature are slightly higher then those of the PT-module at $100^\circ C$.

The module shows a very low dependency of the tail current on the chip temperature compared to the MG100Q2YS9.

In conclusion the ZCS-ARCP in contrast to the ZVS-ARCP is primarily a turn-off snubber. By splitting or by another arrangement of the commutation inductance also a turn-on snubber action is achieved. (The voltage stress on the main switches rises then up to 1.5 times the DC-link voltage.) For the turn-off process at least the major part of the load current is guided away from the main switch;

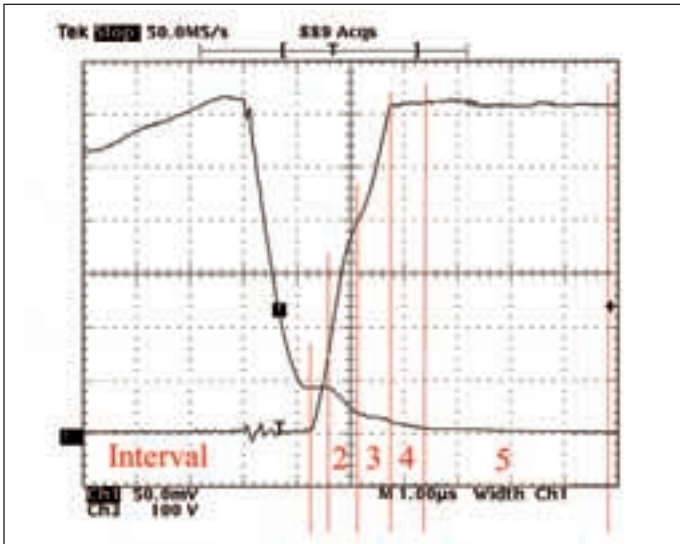


Figure 9: FF150R12KS4 ENG; resonant turn-off, $I_{off} = 80\text{ A}$, $U_{ZK} = 610\text{ V}$, $T_j = 100^\circ\text{C}$

in partial load cases a current in the opposite direction results (quenching). Especially for full load (the load current is commutated down to the level of the tail current) furthermore the rate of rise of the repetitive voltage is reduced, similar to the ZVS action. This explains the especially high snubber action which even rises with increasing load current. The turn-off snubber effect in the full load case is investigated, which depends above all on the tail current behaviour of the power switch. The switching losses are approximately proportional to voltage and current. No noticeable error results due to the conversion

form, e.g., 84A to 80A and 610V to 600V.

In figure 3 it can be seen that the resonant turn-off of the NPT-IGBT has almost no effect on its tail current. For a voltage stress being low as compared to the rated switch voltage the tail losses obviously are increased as compared to the losses during the switching edges. This makes it possible to explain the noticeably decreasing snubber effect with reduced voltage utilisation. The tail losses for the BSM100GB170D result to 8.6mJ and, therefore, are almost equal to the losses resulting for resonant switching.

With a reduction of the resonant frequency of the commutation circuit the obtainable switching frequency (presently about 50kHz) is reduced proportionally. This fact is not compensated by a substantial reduction of the switching losses (tail losses).

The NPT-IGBT in the FF150R12KS4 ENG module shows considerable lower tail losses. Its almost temperature independent tail losses are in the same range as those of the second generation PT IGBT when it is operated at 100°C junction temperature.

In the case of the PT-IGBT the turn-off losses at 600V/80A amount to about 2.3mJ. Com-

leads to 85 percent. Figure 7 represents the turn-off behaviour at full load condition (74A) and room temperature (21°C) of the cooler. The load current is fully commutated, no tail current results. Due to almost negligible switching losses the snubber effect E reaches 100 percent.

The turn-off behaviour of the previous NPT-modules BSM100GB100D and BSM100GB170D from Siemens and the FF150R12KS4ENG from Eupec as well as the second generation PT-module MG100Q2YS1 from Toshiba with equal ZCS-ARCP snubbers are investigated. This snubber reduces simultaneously the di/dt

$I_{off} = 80\text{ A}$, $U_{ZK} = 600\text{ V}$ $T_j = 110^\circ\text{C}$	$W_{off,hard}$ [mJ]	W_{tail} [mJ]	$W_{off,sn}$ [mJ]	E [%]
BSM 100 GB 100 D	14.8	6.1	7.0	52
BSM 100 GB 170 D	14.9	9	9.1	39
MG100Q2 YS9		2.25	2.25	85
MG100Q2 YS9		≈0	≈0	99
FF150R12K S4 ENG		≈0	≈0	99

Table 1: Losses of the modules

pared to the hard switching losses of the NPT-IGBT of about 14.8mJ the snubber effect E

and the du/dt values, in full load operation the remaining turn-off losses are above all influenced by the tail losses. The investigations of the previous NPT IGBTs BSM100GB100D and BSM100GB170D show, that due to the tail current behaviour the snubber effect decreases significantly with decreasing voltage utilisation. The almost temperature independent tail losses of the FF150R12KS4ENG module are in the same range as those of the PT IGBT when it is operated at 100°C junction temperature. The 600V NPT structure is able to compete with the PT structure but it needs an advanced manufacturing technology for thin waver handling. The PT IGBT, operated at 21°C shows almost no tail current, the snubber effect is near 100 percent in this case. ■